

Impact of electron transport layer uniformity on field-induced degradation of inverted perovskite solar cells

**Nikita A. Emelianov, Victoria V. Ozerova, Anastasia A. Bizyaeva,
Mikhail S. Leshchev and Pavel A. Troshin**

General	S2
Figure S1. FTIR spectra for $\text{Cs}_{0.15}\text{FA}_{0.85}\text{PbI}_3/\text{PYF-30}$. Frequency 3271 cm^{-1} , corresponding to N - H stretching vibration in formamidinium cation selected for FTIR-microscopy	S3
Figure S2 FTIR spectra for $\text{Cs}_{0.15}\text{FA}_{0.85}\text{PbI}_3/\text{PC}_{61}\text{BM}$. Frequency 3271 cm^{-1} , corresponding to N - H stretching vibration in formamidinium cation selected for FTIR-microscopy	S3
Figure S3 FTIR spectra for $\text{Cs}_{0.15}\text{FA}_{0.85}\text{PbI}_3/\text{PYF-30}$ with selected for IR s-SNOM microscopy perovskite (1047 cm^{-1}) and ETL (1024 cm^{-1}) frequencies	S4
Figure S4 FTIR spectra for $\text{Cs}_{0.15}\text{FA}_{0.85}\text{PbI}_3/\text{PC}_{61}\text{BM}$ with selected for IR s-SNOM microscopy perovskite (1047 cm^{-1}) and ETL (1738 cm^{-1}) frequencies	S5
Figure S5 AFM phase-contrast images of ETL layers after 1000 hours of field-induced aging	S6

General

All solvents and reagents were purchased from commercial suppliers (Acros Organics, Sigma-Aldrich) and were either used as received or purified using standard methods.

Perovskite solar cells. The perovskite solar cells were assembled in the p-i-n configuration of ITO/PTAA/Cs_xFA_{1-x}PbI₃/ETL/Mg/Ag following the procedure reported previously.^{S1}

FTIR-microscopy measurements. Fourier-transform infrared (FTIR) microscopy (iN-10, Thermo Fisher) were performed in reflection mode. The area 1500×1500 μm was scanned with resolution 50×50 pixels. In each point, 8 spectra were collected.

Infrared scanning near-field microscopy (IR s-SNOM) measurements. The infrared scanning near-field microscopy (IR s-SNOM) (neaSNOM, Neaspec) were performed in PsHet mode with a Mid-IR laser MIRcat-2400 (Daylight Solutions) inside an MBraun glove box. ARROW-NCPt (NANOWORLD, Neuchâtel, Switzerland) cantilevers with PtIr coatings with a probe radius of <25 nm, with a typical resonance frequency of 285 kHz and a stiffness of 42 N m^{-1} were used. The cantilever oscillation amplitude reached 50–65 nm. The area 5×5 μm was scanned with resolution 200×200 pixels with speed 1.5 $\mu\text{m s}^{-1}$.

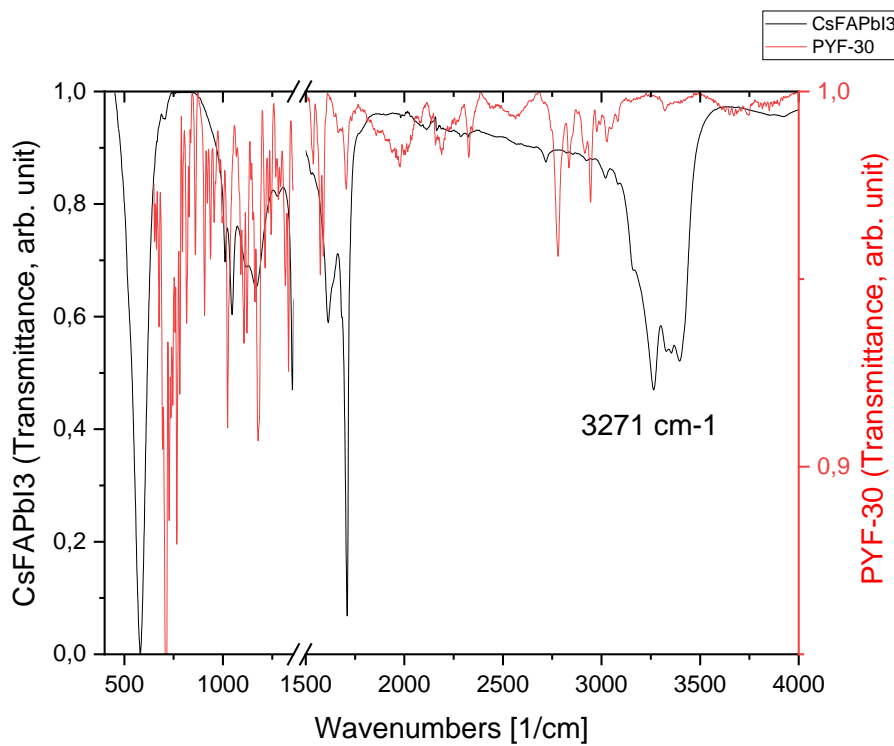


Figure S1 FTIR spectra for $\text{Cs}_{0.15}\text{FA}_{0.85}\text{PbI}_3/\text{PYF-30}$. Frequency 3271 cm^{-1} , corresponding to N-H stretching vibration in formamidinium cation selected for FTIR-microscopy.

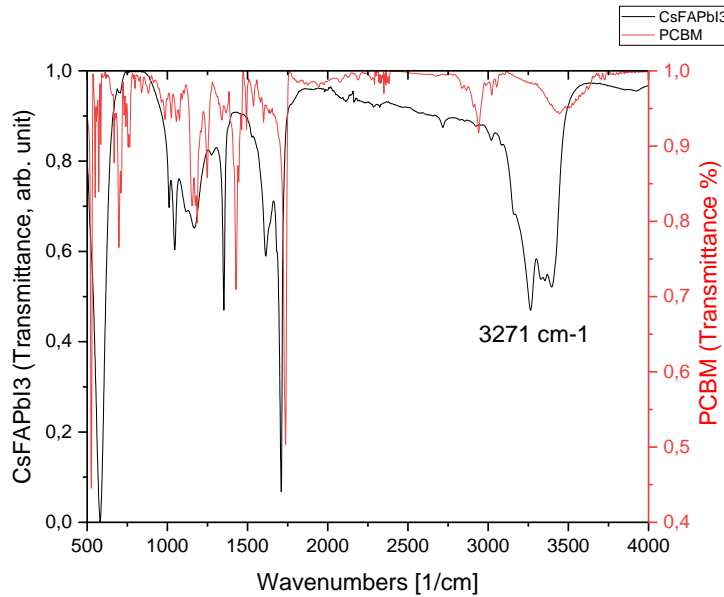
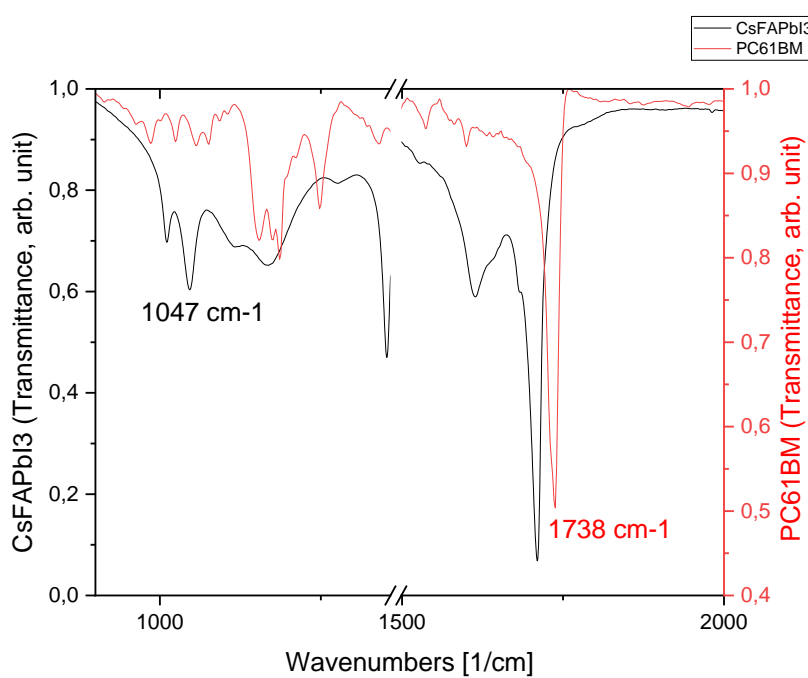
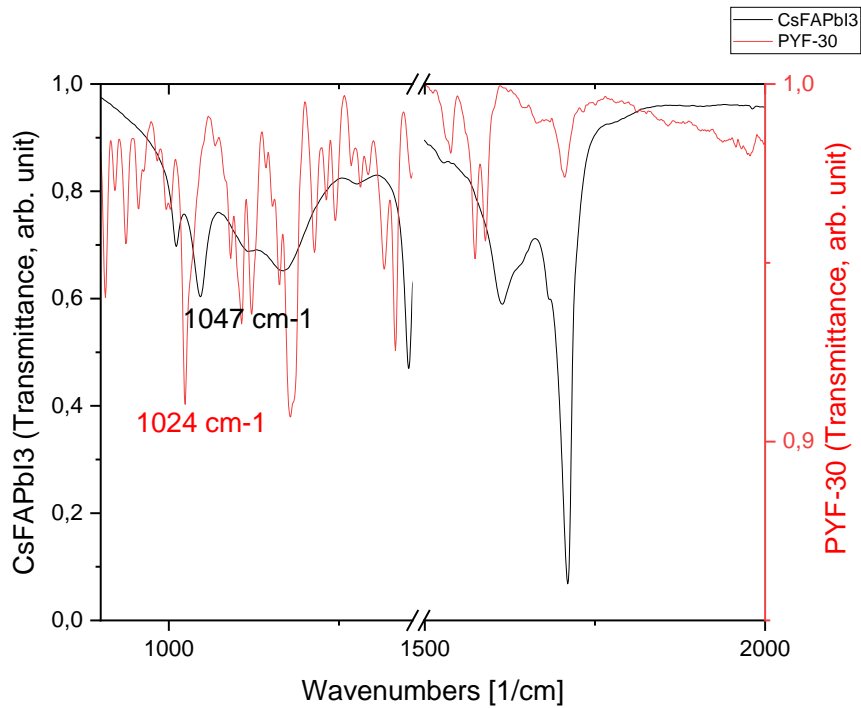


Figure S2 FTIR spectra for $\text{Cs}_{0.15}\text{FA}_{0.85}\text{PbI}_3/\text{PC}_{61}\text{BM}$. Frequency 3271 cm^{-1} , corresponding to N-H stretching vibration in formamidinium cation selected for FTIR-microscopy.



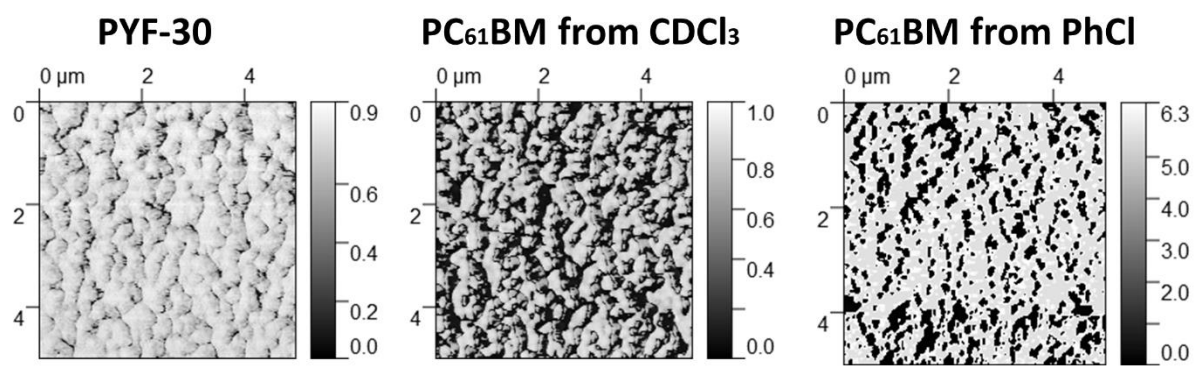


Figure S5 AFM phase-contrast images of ETL layers after 1000 hours of field-induced aging.

Reference

S1 V. V. Ozerova, N. A. Emelianov, L. A. Frolova, Y. S. Fedotov, S. I. Bredikhin, S. M. Aldoshin and P. A. Troshin, *Sustainable Energy Fuels*, 2024, **8**, 997.